ARTICLE
Journal of Cellular Biochemistry 113:590–598 (2012)

Journal of Cellular Biochemistry

Combination of Retinal Pigment Epithelium Cell-Conditioned Medium and Photoreceptor Outer Segments Stimulate Mesenchymal Stem Cell Differentiation Toward a Functional Retinal Pigment Epithelium Cell Phenotype

Chen Huang,[1,2] Jing Zhang,[1] Mingxin Ao,[1] Ying Li,[1] Chun Zhang,[1] Yonggen Xu,[1] Xuemin Li,[1] and Wei Wang[1*]

[1]*Department of Ophthalmology, Peking University Third Hospital, 49 North Garden Road, Haidian District, Beijing 100191, China*

[2]*Medical Research Center, Peking University Third Hospital, 49 North Garden Road, Haidian District, Beijing 100191, China*

ABSTRACT

Recent studies have suggested that bone marrow-derived mesenchymal stem cells (BMMSCs) are capable of retinal tissue-specific differentiation but not retinal pigment epithelium (RPE) cell-specific differentiation. Photoreceptor outer segments (POS) contribute to RPE development and maturation. However, there has been no standard culture system that fosters the differentiation of BMMSCs into mature RPE cells in vitro. In this study, we investigated if the soluble factors from RPE cells and POS could differentiate BMMSCs into cells having a phenotype characteristic of RPE cells. Rat BMMSCs were separately co-cultured with RPE cells, or they were exposed to either control medium, RPE cell-conditioned medium (RPECM), POS, or a combination of RPECM and POS (RPECM-POS). After 7 days, the cells were analyzed for morphology and the expression of RPE markers (cytokeratin 8, CRALBP, and RPE65) to assess the RPE differentiation. Significantly higher pigment accumulation and increased protein expression of the three markers were seen in cells cultured in RPECM-POS than in other treated cultures. Furthermore, the RPECM-POS-treated cultures displayed ultrastructural features typical of RPE cells, expressed RPE cell functional proteins, and had the capability to phagocytose POS. Together, theses results suggest the combination of RPECM and POS stimulate BMMSCs differentiation toward a functional RPE phenotype. Our results provide the foundation for a new route to RPE regenerative therapy involving BMMSCs. Future work isolating the active agent in RPECM and POS would be useful in therapies for RPE diseases or in developing appropriately pre-differentiated BMMSCs for tissue-engineered RPE reconstruction. J. Cell. Biochem. 113: 590–598, 2012.

KEY WORDS: MESENCHYMAL STEM CELLS; RETINAL PIGMENT EPITHELIUM; CONDITIONED MEDIUM; PHOTORECEPTOR OUTER SEGMENT; DIFFERENTIATION

Retinal pigment epithelium (RPE) dysfunction leads to many devastating retinal diseases, such as age-related macular degeneration (AMD) and retinitis pigmentosa (RP), which are the leading causes of permanent visual loss in humans [van Soest et al., 1999]. Currently, the effective treatment for severe retinal diseases is RPE transplant. Autologous RPE, harvested from the midperiphery, has been transplanted as a cell suspension or as a patch of RPE and choroid in AMD patients [Joussen et al., 2006]. However, a critical shortage of transplant-ready RPE cells limits this approach, highlighting the need to develop renewable sources of replacement cells.

Bone marrow-derived mesenchymal stem cells (BMMSCs) have been proposed as a potential individual cellular source for replacement therapies aimed at treating degenerative diseases.

Additional Supporting Information may be found in the online version of this article.

Grant sponsor: National Natural Science Foundation of China; Grant number: 30672284; Grant sponsor: China Postdoctoral Science Foundation; Grant number: 20080430288.

*Correspondence to: Wei Wang, Department of Ophthalmology, Peking University Third Hospital, 49 North Garden Road, Haidian District, Beijing 100191, China. E-mail: puh3_ww@bjmu.edu.cn

Received 8 May 2011; Accepted 16 September 2011 • DOI 10.1002/jcb.23383 • © 2011 Wiley Periodicals, Inc.
Published online 21 September 2011 in Wiley Online Library (wileyonlinelibrary.com).

Previous studies indicated that BMMSCs have the ability to differentiate beyond tissues of dermal origin into retinal tissue cells in vitro and in vivo. Using the co-culture system with RPE cells, BMMSCs differentiated into retina-specific cells and expressed several retina-specific markers, including photoreceptor marker opsin [Chiou et al., 2005] and RPE cell markers cytokeratin, RPE65, and microphthalmia transcription factor (MITF) [Li et al., 2007]. Transplanted BMMSCs have migrated and incorporated into the retinal injury site, initiated retinal tissue repair, and expressed functional proteins of the retina [Atmaca-Sonmez et al., 2006; Harris et al., 2006; Li et al., 2006, 2007; Arnhold et al., 2007; Castanheira et al., 2008; Gong et al., 2008]. However, the retinal differentiation of BMMSCs represents the tissue-specificity rather than cell-specificity using co-culture system and injection. There still remains the difficulty in obtaining a specific population of the BMMSCs-derived RPE cells.

The microenvironment of a cell has been implicated as important directors of stem cell differentiation [Ohlstein et al., 2004]. By combining parameters such as the extracellular matrix, culture conditions, and temporally administered growth factors, cell fate can be manipulated in the laboratory [Pittenger et al., 1999; Derda et al., 2007].

The development of the RPE is the result of an interaction between RPE cells and the photoreceptor outer segments (POS). POS are the membranous organelles that extend from photoreceptors and are essential to the last maturation steps of RPE development [Raymond and Jackson, 1995; Marmorstein et al., 1998; Marmorstein, 2001]. The RPE responds by elongating the apical microvilli to surround the POS, and then the RPE and photoreceptors interact to drive the final steps of maturation. Additionally, the shed POS from photoreceptors are phagocytosed by the RPE, an important function of the RPE in the maintenance of retinal metabolism.

The fundamental premise of this study is that RPE differentiation from BMMSCs is similar to RPE development, with the corollary that the microenvironment in which RPE cells grow and mature is likely to be an important contributor to the process of RPE differentiation. We hypothesized that RPE cell-conditioned medium (RPECM) and POS would promote the differentiation of BMMSCs toward a general RPE phenotype, producing cells with characteristics similar to those of cultured RPE cells. The active agent in RPECM and POS would be isolated to use in therapies for RPE diseases or in developing appropriately pre-differentiated BMMSCs for tissue-engineered RPE reconstruction.

MATERIALS AND METHODS

ANTIBODIES

Antibodies against CRALBP (clone D-10, dilution 1:100), RPE65 (clone H-85, dilution 1:100), and MerTK (clone M-217, dilution 1:100) were obtained from Santa Cruz Biotechnology (Santa Cruz, CA). Antibodies against cytokeratin 8 (CK8, clone E2, dilution 1:200), Na^+/K^+ ATPase α-1 (clone C464.6, dilution 1:100), ezrin/radixin/moesin (dilution 1:100), glial fibrillary acidic protein (GFAP, dilution 1:100), and pigment epithelium derived factor (PEDF, clone 10F12.2, dilution 1:100) were obtained from Millipore (Billerica, MA). Antibodies against β-actin (dilution 1:1,000), integrin αVβ5 (clone P1F6, dilution 1:100), tyrosinase (clone EP1577Y, dilution 1:100), N-cadherin (dilution 1:100), and CD36 (clone FA6-152, dilution 1:100) as well as tetramethylrhodamine iso-thiocyanate (TRITC)-conjugated goat anti-mouse IgG (dilution 1:100), TRITC-conjugated goat anti-rabbit IgG (dilution 1:100), Cy5-conjugated goat anti-mouse IgG (dilution 1:100), horseradish peroxidase (HRP)-conjugated goat anti-rabbit IgG (dilution 1:3,000), and HRP-conjugated goat anti-mouse IgG (dilution 1:3,000) were obtained from Abcam (Cambridge, UK).

EXPERIMENTAL ANIMALS

Fifteen Brown-Norway (BN) rats weighing 200–250 g were obtained from Vital River Laboratory Animal Technology Co., Ltd. (Beijing, China) for the isolation of BMMSCs and RPE cells. These animals were handled according to the Association for Research in Vision and Ophthalmology (ARVO) Statement for the Use of Animals in Ophthalmic and Vision Research. All procedures were approved by Peking University's Institutional Animal Care and Use Committee.

ISOLATION AND EXPANSION OF RAT BMMSCs

Rat BMMSCs were harvested from the bone marrow of ten femurs of five BN rats. BMMSCs were plated in complete Dulbecco's Modified Eagle Medium (low glucose) (D-MEM-LG, Invitrogen, Carlsbad, CA) containing 10% fetal bovine serum (FBS, Invitrogen) and 100 units/ml penicillin/streptomycin (Si0gma–Aldrich, St. Louis, MO). The cells were grown at 37°C and 5% CO_2 for 24 h before the medium was replaced to discard nonadherent hematopoietic cells. Adherent BMMSCs were further cultured in medium replaced every 2 days. BMMSCs were used at passage two (P2) for the experiments. At least three independent experiments were performed in duplicate.

FLOW CYTOMETRY ANALYSIS

The cell surface phenotype of P2 BMMSCs were characterized using PE/Cy7 anti-rat CD45 and PE anti-mouse/rat CD29 (BioLegend, San Diego, CA) using a standard fluorescence-activated cell sorting (FACS) analysis. The cells were analyzed with a FACScan (BD Biosciences, San Jose, CA), and the data were analyzed with the CellQuest software (BD Sciences). At least three independent experiments were performed in duplicate.

OSTEOGENIC AND ADIPOGENIC DIFFERENTIATION FROM BMMSCs

The osteogenic differentiation medium included 10 mM β-glycerophosphate, 50 μg/ml ascorbic acid, and 10 nM dexamethasone in the complete D-MEM/F-12 culture medium described above. For adipogenic differentiation, 1 μM dexamethasone, 0.5 mM 3-isobutyl-1-methylxanthine (IBXM), 10 μg/ml insulin, and 100 μg/ml indomethacin were added to the complete D-MEM/F-12 medium. All of these supplemental compounds or reagents were obtained from Sigma–Aldrich. Cells were cultured for 4 weeks for osteogenic differentiation or for 2 weeks for adipogenic differentiation. Osteogenic differentiation was confirmed by von Kossa staining, and adipogenic differentiation was confirmed by Oil Red O staining. At least three independent experiments were performed in duplicate.

ISOLATION AND EXPANSION OF RAT RPE CELLS

Rat RPE cells were isolated using a modification of a previously described method [Chang et al., 1991]. RPE cells were harvested from ten eye cups of five BN rats. The eye cups were incubated in 215 units/ml hyaluronidase (Sigma–Aldrich) and 0.125% trypsin-0.01% EDTA (Invitrogen) for 5 min. The retina was gently stripped. The RPE were incubated in 0.25% trypsin-0.02% EDTA (Invitrogen) for 30 min and detached from the choroid by mechanical dissociation using a pipette. The dissociated cells were separated by centrifugation for 10 min at 1,000 rpm and resuspended in complete D-MEM/F-12 medium containing 10% FBS, 100 units/ml penicillin/streptomycin. The harvested cells were seeded at a density of 3×10^4 cells/cm^2 in 100-mm culture dishes and grown at 37°C and 5% CO_2. RPE cells were used at passage one (P1) as the control for the experiments. At least three independent experiments were performed in duplicate.

PREPARATION OF RPECM

The culture medium of P0–P2 RPE cells was collected every 2 days until full confluence was reached for collecting the supernatant. The starting cell density of the resulting RPECM was 1×10^5 RPE cells/ml medium. RPECM was filtered through a membrane to remove the cells and stored at −20 °C.

PREPARATION OF RAT AND PORCINE POS

Rat POS derived from BN rats and porcine POS obtained from a local abattoir (Beijing, China) were isolated according to the method of Hall and colleagues [Hall, 1978]. The retinal tissue was gently stirred for 30 min in a cold 0.25% trypsin-0.02% EDTA solution with a magnetic stirrer at 4°C. Large tissue fragments were eliminated by precipitation at 4°C for 20 min, and supernatants were centrifuged at 1,000 rpm for 10 min. The samples were washed three times with fresh PBS, resuspended in D-MEM/F-12 to a concentration of 1×10^{10} ml^{-1}, and stored at −80°C until use.

RPE DIFFERENTIATION OF BMMSCs

BMMSCs consisting of approximately 2×10^5 cells were plated in 6-well plates and incubated overnight in complete D-MEM/F-12 medium (control medium, CM). The cells were then assigned to one of five groups: CM, S-Co (separately co-cultured with 2×10^5 RPE cells using the Millicell cell culture insert system), RPECM (RPECM 1:4 dilution with CM), POS (CM with 1×10^8 POS/ml), or RPECM-POS (a combination of RPECM and POS). For all groups, the culture medium was changed every 2 days. The cells were grown at 37°C and 5% CO_2 for 7 days for the RPE differentiation experiment. At least three independent experiments were performed in duplicate.

IMMUNOCYTOCHEMISTRY

Cells were washed three times with PBS and fixed with 4% paraformaldehyde for 15 min at 4°C. The cells were blocked in 10% goat serum for 30 min and then incubated in primary antibody diluted in 0.5% bovine serum albumin (BSA) at 37°C for 2 h. At the end of the incubation period, the cells were washed three times with PBS and incubated with secondary antibodies for 45 min at 37°C. Nuclei were stained with DAPI (1:1,000, Sigma–Aldrich). Stained samples were visualized by fluorescence microscopy (Nikon) and quantified using Image Pro Plus 5.0 (Media Cybernetics, Bethesda, MD). At least three independent experiments were performed in duplicate.

WESTERN BLOTTING

Cells were lysed, and their protein concentrations were determined using a BCA protein assay (Pierce, Rockford, IL). The cell lysates (50 μg of protein per lane) were separated by 10% sodium dodecyl sulfate–polyacrylamide gelelectrophoresis (SDS–PAGE) and were transferred to nitrocellulose membranes (Hyclone, Logan, UT). The membranes were blocked with 5% (v/v) skim milk and probed with primary antibodies against RPE65, CRALBP, CK8, and beta-actin at 4°C overnight. Following washing, the membranes were incubated with HRP-conjugated secondary antibodies at room temperature for 1 h. The bound antibodies were visualized using an ECL system (Amersham Pharmacia Biotech, Piscataway, NJ). At least three independent experiments were performed in duplicate.

SCANNING ELECTRON MICROSCOPY (SEM)

Cells grown on the coverslips were fixed in 2% glutaraldehyde in PBS for 2 h at room temperature, washed three times with PBS, and then dehydrated through a graded series of ethanol, 25%, 50%, 75%, 90%, 95%, and twice at 100% for 20 min each before processing. Samples were mounted on aluminum stubs, sputter-coated with gold-palladium, and examined using SEM (S-800; HITACHI Ltd., Hitachinaka, Japan). At least three independent experiments were performed in duplicate.

TRANSMISSION ELECTRON MICROSCOPY (TEM)

Cells were washed three times with PBS and scraped with a cell scraper (Corning, NY). Samples were centrifuged at 800 g for 10 min, removed the supernatant PBS, fixed with 2% glutaraldehyde in PBS for 2 h at room temperature, washed three times in PBS for 5 min per wash, and then dehydrated through a graded series of ethanol and embedded in Epon 812. Ultrathin (90-nm) sections were collected on copper grids and double-stained with uranyl acetate and lead citrate and then examined using transmission electron microscopy (TEM) (H-7100, HITACHI Ltd.). At least three independent experiments were performed in duplicate.

RNA EXTRACTION AND REVERSE TRANSCRIPTASE-POLYMERASE CHAIN REACTION (RT-PCR)

Total RNA was isolated using TRIzol (Invitrogen) following the manufacturers' protocol. Total RNA (5 μg) was transcribed by reverse transcriptase (RevertAidTM First Strand cDNA Synthesis Kit, Fermentas, Glen Burnie, MD) and used for PCR using PCR Master Mix (2X) (Fermentas). Primers were used for detecting the following genes: Na^+/K^+ ATPase, MerTK, bestrophin 1, ezrin, tyrosinase, RPE65, PEDF, and GAPDH. Primer sequences are listed in Table I.

PHAGOCYTOSIS ASSAY

Porcine POS were labeled with the fluorescein isothiocyanate (FITC) method described by Lutz and Lin [Lutz et al., 1995; Lin and Clegg, 1998]. Briefly, the porcine POS were suspended in 10 ml PBS containing 20 μM FITC (Sigma–Aldrich) overnight in the dark at

TABLE I. Primer Sequences Used for Reverse Transcriptase–Polymerase Chain Reaction

Gene	Primer sequence	Product (bp)
Na^+/K^+ ATPase	F: 5′-CGAAATGGAGAGAAGATGAG-3′ R: 5′-ACCAATGAGGAAGATGACAG-3′	462
MerTK	F: 5′-AAAAGGAGAGTCCAGGAAAC-3′ R: 5′-TCCATTACAGACCCAAACTC-3′	233
Bestrophin 1	F: 5′-GGGAATATAAGCAGTTGCAG-3′ R: 5′-CCAGTTGGTCTCAAAATCAT-3′	431
Ezrin	F: 5′-ACCTGGCTGAAACTTGATAA-3′ R: 5′-ATAGCACTGTCCTTGAGCAT-3′	395
Tyrosinase	F: 5′-AGACTGTGCCTCCTCTAAG-3′ R: 5′-TTGCCAAAGTGAGGTAAG-3′	359
RPE65	F: 5′-ACAACTGCCACAGCCATTC-3′ R: 5′-CCAGGACTCACCACCACA-3′	317
PEDF	F: 5′-CTGGCAACCCTCGCATAG-3′ R: 5′-TGTCCTCGTCCAAGTGAAA-3′	201
GADPH	F: 5′-TATCGGACGCCTGGTTAC-3′ R: 5′-TGCTGACAATCTTGAGGGA-3′	407

F, forward primer; R, reverse primer. GADPH was used as inner control.

4°C. FITC-labeled porcine POS were washed five times with fresh PBS and resuspended in D-MEM/F-12 to a concentration of 1×10^8 POS/ml. The cultured cells were incubated with 10^7 labeled POS/ml for 3, 10, or 24 h at 37°C in 5% CO_2. After the incubation, the cells were gently washed four to five times with 37°C PBS to remove unbound POS. The fluorescence of bound FITC-POS was quenched by 0.2% trypan blue in PBS, and the fluorescence level of internalized POS was determined. Nuclei were stained with DAPI (1:1,000). At least five different areas of each well were assessed. Duplicate wells were used for each experimental condition. The porcine POS internalization was quantified using Image Pro Plus 5.0. At least three independent experiments were performed in duplicate.

STATISTICS

All data represent the mean ± SE from at least three independent experiments. Statistical analysis of the data was performed using ANOVA. $P < 0.05$ was considered significant.

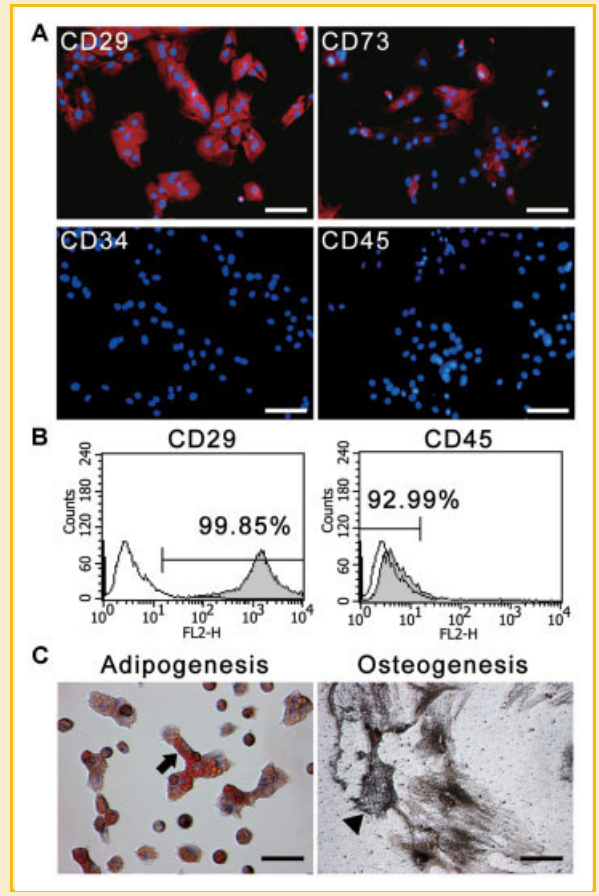

Fig. 1. Characteristics of rat BMMSCs. A: Immunofluorescence staining for CD29, CD73, CD34, and CD45. B: Flow cytometry analysis of CD29 and CD45. C: Adipogenic (left) and osteogenic differentiation (right) of BMMSCs. Black arrow indicates oil inclusions confirmed by Oil Red O staining. Black triangle indicates calcium deposits confirmed by von Kossa staining. Scale bar = 50 μm in (A) and (C). All experiments were repeated at least three times with similar results. [Color figure can be seen in the online version of this article, available at http://wileyonlinelibrary.com/journal/jcb]

RESULTS

CHARACTERISTICS OF RAT BMMSCs

At P0 and P1, rat BMMSCs were morphologically heterogeneous. From P2, BMMSCs became morphologically homogenous and had a fibroblast-like phenotype. To determine the multipotent potential of BMMSCs, the immunological and functional characteristics of P2 BMMSCs were assessed. BMMSCs were positive for CD29 and CD73 but were negative for the hematopoietic lineage markers CD34 and CD45 (Fig. 1A and B). In addition, BMMSCs were capable of differentiating into adipocytes and osteocytes, which were demonstrated by Oil Red O staining and von Kossa staining, respectively (Fig. 1C).

RAT RPE CELLS CULTURE

Rat RPE cells in primary culture adopted the typical polygonal morphology associated with intact RPE and possessed pigment granules. As shown in Figure 2, subcultured P1 RPE cells were elongated and took on the appearance of fibroblast-like pigment cells. The pigment granules were lost from the RPE cells in the RPECM at later passages as a result of dilution by cell division. At passage 3, the RPE cells lost their morphological appearance of pigment cells but showed no decrease in viability (data not shown). These observations suggest that the P0–P2 RPE cells retained viability as well as their functional phenotype in culture. Thus, the RPECM collected from P0–P2 RPE cells was a valid reagent for testing the biological activity of the secreted products of RPE cells.

MORPHOLOGICAL CHANGES IN BMMSCs AFTER INDUCTION

We next examined the effects of the separate co-culture system with RPE cells (S-Co), exposure to RPECM, POS, or a combination of RPECM and POS on the differentiation activities of BMMSCs compared with CM. The morphological changes were observed every day under a phase-contrast microscope.

After incubation in the various media for 7 days, the cytoplasmic pigment granules were enhanced in both the RPECM- and

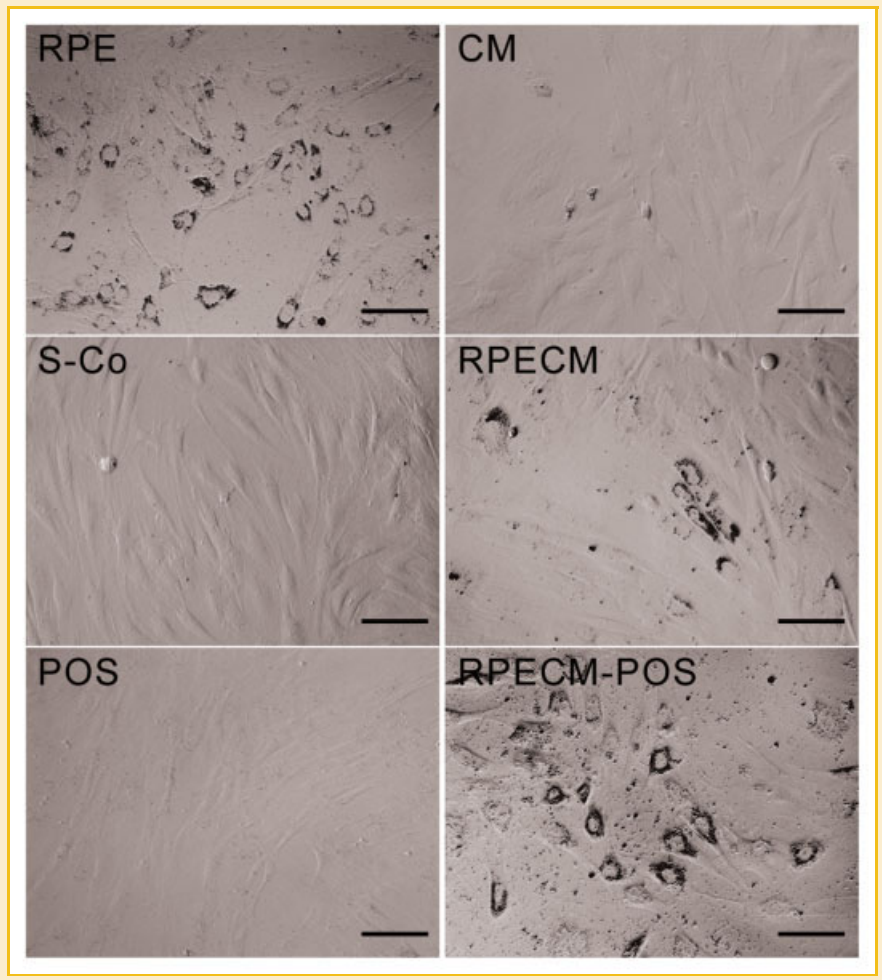

Fig. 2. Morphology in P1 RPE cells and BMMSCs cultures treated with CM, S-Co, RPECM, POS, or RPECM-POS. The RPE differentiation of BMMSCs was induced in either the S-Co system, in culture medium containing RPECM, POS, or a combination of RPECM and POS. The morphologies of the cultures were observed using phase contrast microscopy after 7 days of treatment. All experiments were repeated at least three times with similar results. Scale bars = 100 μm. [Color figure can be seen in the online version of this article, available at http://wileyonlinelibrary.com/journal/jcb]

RPECM-POS-treated cultures (similar to cultured P1 RPE cells) with RPECM-POS treatment being significantly more effective than RPECM treatment (Fig. 2). However, the polygonal cells typical of primary RPE cells were totally absent after incubation for 7 days (data not shown). Interestingly, the pigment granules exocytosed by cultured RPE cells were confined in the Millicell cell culture inserts of the separate co-culture system, and they did not enter into the underlying BMMSCs culture. The morphology of the BMMSCs in S-Co treated cultures did not change significantly. The cytoplasmic vacuoles rather than the pigment granules were enhanced in POS-treated cultures. It was worth noting that the cellular density of BMMSCs cultured in RPECM-POS was less than that of the cells cultured in CM, S-Co, RPECM, or POS.

EXPRESSION OF THE RPE CELL-SPECIFIC MARKERS CK8, CRALBP, AND RPE65 IN TREATED BMMSCs

We examined the protein expression levels of CK8 (an indicator of epithelial cells), CRALBP, and RPE65 (crucial factors in the maintenance of photoreceptor visual cycles) at day 7 of culture to assess and compare the differentiation response of BMMSCs to the different treatments. As shown in Figure 3, the S-Co system, RPECM, POS, and RPECM-POS had distinct effects on the expression levels of CK8, CRALBP, and RPE65 protein relevant to RPE cell phenotype.

As shown in Figure 3, protein expression of CK8, CRALBP, and RPE65 was clearly detected in P1 RPE cells, but not in BMMSCs cultured in CM. CK8-positive cells and CRALBP-positive cells were present in differentiated treated cultures, with RPECM-POS treatment (100% and 100%, respectively) being significantly more effective than S-Co ($17 \pm 2\%$ and $16 \pm 2\%$, respectively), RPECM ($86 \pm 3\%$ and $75 \pm 4\%$, respectively), and POS ($21 \pm 1\%$ and $89 \pm 2\%$, respectively) treatment. However, RPE65-positive cells were detected in RPECM-POS ($83 \pm 3\%$), RPECM ($26 \pm 3\%$), and POS ($22 \pm 4\%$) treatment but rarely seen in S-Co treated cultures. Moreover, protein expression levels of CK8, CRALBP, and RPE65 were significantly up-regulated in RPECM-POS versus other differentiated treated cultures (Fig. 3B).

These observations suggest that the combination of RPECM and POS had strong effects on the promotion of BMMSCs toward the RPE phenotype. Thus further studies on the cellular ultrastructure, the

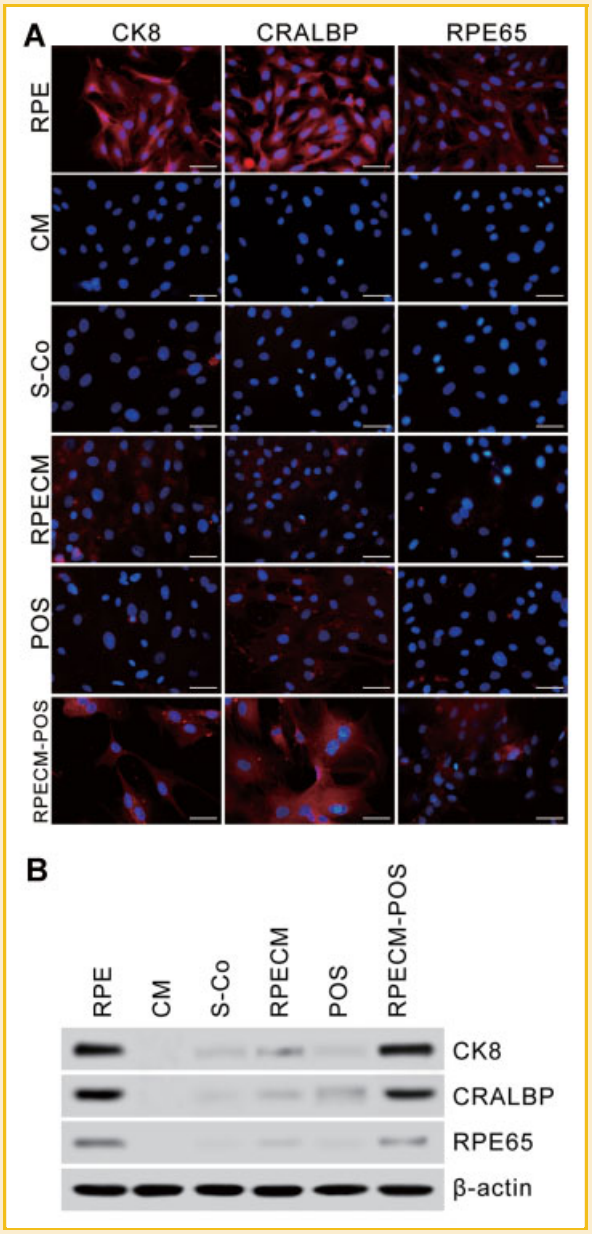

Fig. 3. The expression of RPE-specific markers CK8, CRALBP, and RPE65 in P1 RPE cells and BMMSCs cultures treated with CM, S-Co, RPECM, POS, or RPECM-POS. A: Immunofluorescence staining for CK8, CRALBP, and RPE65 proteins. Cultures were examined after 7 days of treatment. Cell nuclei were stained with DAPI. Scale bars = 50 μm. B: The expression of CK8, CRALBP, and RPE65 proteins detected using Western blotting. β-actin was used as a loading control. All experiments were repeated at least three times with similar results. [Color figure can be seen in the online version of this article, available at http://wileyonlinelibrary.com/journal/jcb]

expression of RPE functional markers, and the activity of functional phagocytosis in the RPECM-POS-treated cultures were performed to assess the state of RPE differentiation.

ULTRASTRUCTURE OF RPECM-POS-TREATED CULTURES

We next confirmed the ultrastructural features of the RPECM-POS treated cultures using SEM and TEM. As shown in Figure 4, the cells in the RPECM-POS-treated cultures showed an apical surface covered by a dense carpet of microvilli. POS were bound to the microvilli-rich surface of the cell (Fig. 4A), and had been ingested or were in the process of being engulfed by the cell (Fig. 4B). Another specific feature was the appearance of numerous dark-staining pigment granules that were prominent in the cytoplasm of the cells in the RPECM-POS-treated cultures (Fig. 4B).

EXPRESSION OF RPE FUNCTIONAL MARKERS IN RPECM-POS-TREATED CULTURES

To determine whether the RPECM-POS-treated cultures possess the RPE functional characteristics, the protein and mRNA expressions of genes known to be associated with RPE function were examined by immunofluorescence and RT-PCR. As shown in Figures 5 and 6, the RPECM-POS-treated cultures showed strong expression of RPE functional markers, such as the apical polarization protein Na^+/K^+ ATPase [Jaitovich and Bertorello, 2006], regulators of phagocytosis CD36, integrin αVβ5 [Finnemann and Silverstein, 2001], and MerTK [Gal et al., 2000], the melanin synthetic enzyme tyrosinase [Jaitovich and Bertorello, 2006], and calcium-activated Cl^- channel bestrophin-1 [Rosenthal et al., 2006]. The expression levels were the same as the protein and/or mRNA levels in P1 RPE cells. In contrast, there was no obvious expression of these proteins in the BMMSCs treated with CM except for low levels of expression of apical polarization protein ezrin. Interestingly, ezrin, which is required for the development of long apical microvilli [Bonilha and Rodriguez-Boulan, 2001], and cellular adherens junction (N-cadherin) [Youn et al., 2006] were more highly expressed in the RPECM-POS-treated cultures than in the P1 RPE cells. PEDF was expressed in all cell types tested, but its expression levels in the RPECM-POS-treated cultures were closer to the P1 RPE cells than the level in the CM-treated cultures. The glial marker GFAP was absent in P1 RPE cells, CM- and RPECM-POS-treated cultures.

FUNCTIONAL PHAGOCYTOSIS ACTIVITY OF POS IN RPECM-POS TREATED CULTURES

Phagocytosis of POS is one of the functions of RPE cells in vivo [Hall, 1978]. FITC-labeled porcine POS were used to investigate the functional phagocytosis activity in the RPECM-POS-treated cultures. The levels of fluorescence density were measured to evaluate the phagocytic activity in P1 RPE cells, CM- and RPECM-POS-treated cultures. As shown in Figure 7A, after the fluorescence of bound FITC-POS was quenched by trypan blue, the internalized FITC-labeled POS were present in both RPE cells and RPECM-POS-treated cultures, but not in CM-treated cultures. A time course analysis (Fig. 7B) showed that a higher fluorescence density persisted at all times tested (3, 10, and 24 h), indicating that RPECM-POS-treated cultures possessed similar phagocytic activity as P1 RPE cells in vitro.

DISCUSSION

In this study, we examined the effects of RPECM and POS on the differentiation response of multipotent BMMSCs in comparison with the response of BMMSCs to control medium or separately co-

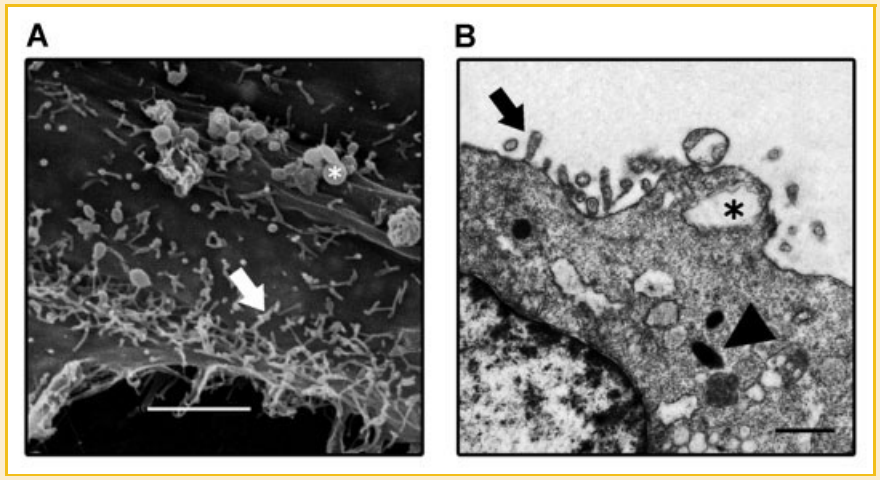

Fig. 4. Ultrastructure of RPECM-POS treated cultures. A: Scanning electron microscopy. White arrow indicates microvilli, and white asterisk denotes bound POS on the cellular surface. B: Transmission electron microscopy. Black arrow indicates microvilli on the cellular surface. Black triangle indicates pigment granules, and black asterisk denotes ingested POS in the cytoplasm. Scale bar = 5-m in (A), 1-m in (B). All experiments were at least repeated three times with similar results.

cultured with RPE cells. Consistent with our hypothesis, the combination of RPECM and POS significantly promoted an RPE phenotype in BMMSCs that was distinct from that observed in the cultures treated with the separate co-culture system with RPE cells, RPECM or POS. Phenotypic characteristics of RPECM-POS-treated cultures were reminiscent of RPE differentiation, including the cytoplasmic pigment granules and significantly higher levels of CK8, CRALBP, and RPE65 expression compared with other treated cultures. In addition, the RPECM-POS-treated cultures displayed typical RPE ultrastructural features, expressed RPE functional molecules associated with apical polarization, phagocytosis, melanization, and cellular adherens junctions, and had the capability to functionally phagocytose POS. Taken together, these results suggest that the combination of RPECM and POS has the potential to differentiate BMMSCs towards the RPE phenotype.

Retinal differentiation from BMMSCs in vitro has been studied for 7 years [Chiou et al., 2005; Li et al., 2007], but no standard culture system exists for the differentiation of BMMSCs into mature RPE cells in vitro. Previous study has shown that using the direct contact co-culture system with RPE cells, BMMSCs expressed markers of the RPE lineage by day 14 ($89 \pm 6\%$ expressed cytokeratin, $80 \pm 11\%$ expressed MITF, and $81 \pm 13\%$ expressed RPE65) [Li et al., 2007].

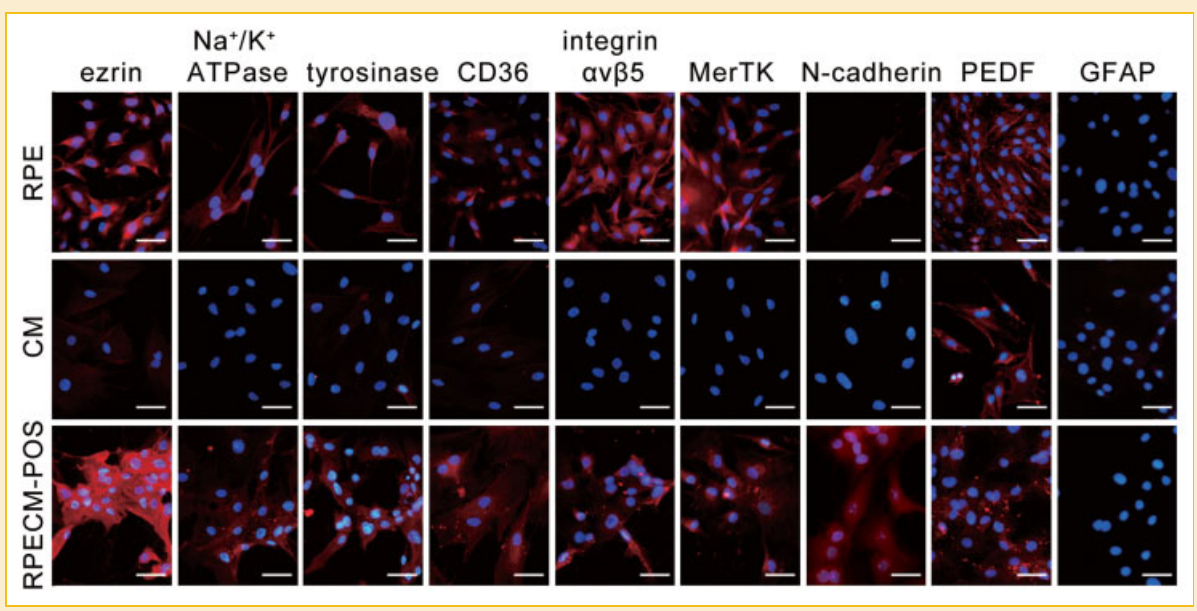

Fig. 5. Immunofluorescence analysis of the RPE functional markers ezrin, Na^+/K^+ ATPase, CD36, integrin $\alpha v\beta 5$, MerTK, N-cadherin and PEDF, and expression analysis of the glial cell marker GFAP in P1 RPE cells, CM- and RPECM-POS-treated cultures. Cultures were examined after 7 days of treatment. Cell nuclei were stained with DAPI. Scale bar = 50 μm. All experiments were repeated at least three times with similar results. [Color figure can be seen in the online version of this article, available at http://wileyonlinelibrary.com/journal/jcb]

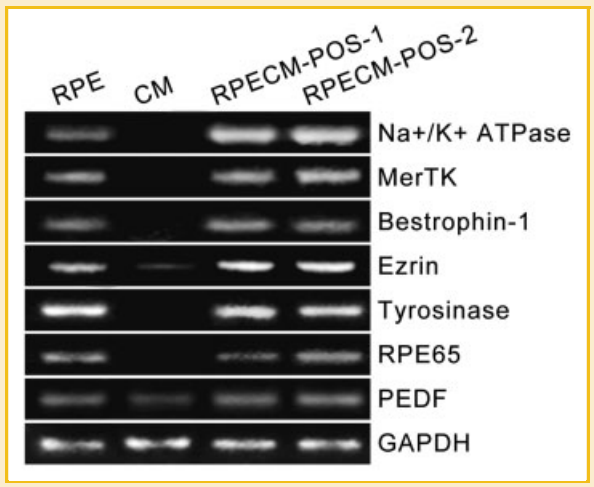

Fig. 6. RT-PCR analysis of RPE functional marker genes Na^{+}/K^{+} ATPase, MerTK, bestrophin-1, ezrin, tyrosinase, RPE65, PEDF expressions in P1 RPE cells, CM- and RPECM-POS-treated cultures. Cultures were examined after 7 days of treatment. RPECM-POS-1 and RPECM-POS-2 indicate the RPECM-POS-treated cultures derived from two independent experiments. GAPDH was served as sample loading control. All experiments were repeated at least three times with similar results.

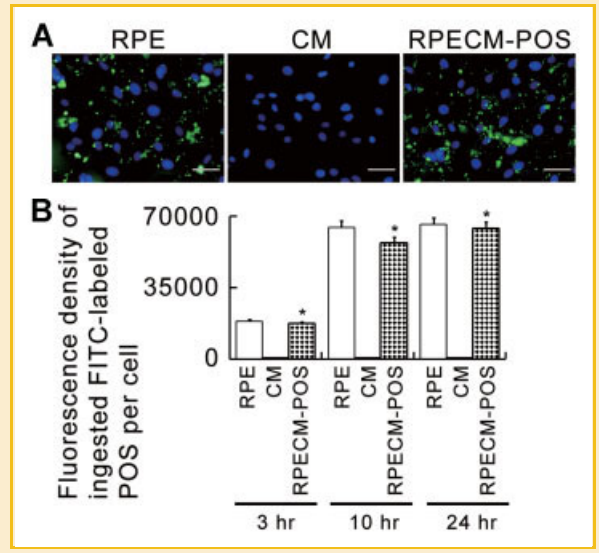

Fig. 7. Functional phagocytosis activity of POS in P1 RPE cells, CM- and RPECM-POS-treated cultures. Cultures were examined after 7 days of treatment. A: Fluorescence microscopy of ingested FITC-labeled POS in P1 RPE cells, CM- and RPECM-POS-treated cultures incubated for 24 h and quenched with trypan blue. Cell nuclei were stained with DAPI. Scale bar = 50 μm. B: Quantitative analysis of ingested FITC-labeled POS in cells. Data were averaged from three independent experiments. Each bar represents the mean ± SD. An asterisk indicates significantly greater fluorescence density in RPECM-POS-treated cultures relative to CM-treated cultures ($P < 0.05$). [Color figure can be seen in the online version of this article, available at http://wileyonlinelibrary.com/journal/jcb]

However, these effects were abolished when the BMMSCs were separated by a semipermeable membrane and were not in direct cell–cell contact with the RPE.

Here, we differentiated BMMSCs into cells with an RPE phenotype by incubating them in different artificial microenvironments imitating RPE development in vivo. The RPE differentiation state of the BMMSCs was characterized morphologically and based on the expression of RPE markers in accordance with current scientific knowledge. Pigmentation is a unique parameter indicating RPE cell maturation, though the propagation of RPE cells in culture causes loss of their pigments [Alge et al., 2003]. CK8, an epithelial cell marker, has been detected in all RPE cultures [Hunt and Davis, 1990]. Similarly, CRALBP and RPE65, which are crucial for the maintenance of photoreceptor visual cycles and required for regeneration of visual pigments by photoreceptors, are also expressed in RPE cells [Huang et al., 2009]. RPE65 protein is a rate-limiting enzyme for the visual cycle and becomes undetectable after two to three passages of RPE cell culture [Alge et al., 2003]. Therefore, in terms of use in clinical therapy, the RPE differentiated cells with the persistent expression of RPE65 offer significant advantages. In the present study, we demonstrated that the combination of RPECM and POS have the compelling capacity to differentiate BMMSCs toward an RPE phenotype with enhanced cytoplasmic pigment granules and clear expression of CK8, CRALBP, and RPE65. The results of ultrastructural analysis, RPE functional marker expression measurements, and functional phagocytosis activity assessment further confirmed the effective RPE differentiation achieved through the combination of RPECM and POS.

The cell culture inserts of the separate co-culture system or the conditioned medium were used to investigate stem cell differentiation based on the secretion of soluble factors. It was worth noting that the conditioned medium of RPE cells included not only the soluble factors but also the pigment granules that were exocytosed by cultured RPE cells. However, the pigment granules were confined in the RPE cultured inserts of the separate co-culture system and did not affect the underlying BMMSCs culture. The more effective RPE differentiation achieved with RPECM treatment as opposed to the separate co-culture system suggested that the pigment granules may have contributed to the RPE differentiation of BMMSCs. POS, the essential factor for RPE maturation, has been added to RPE cultures to increase the pigment content of RPE cells [Rakoczy et al., 1992]. Our study revealed that simple stimulation of POS was insufficient to accelerate the pigment formation in BMMSCs or to promote the appearance of the epithelial phenotype of RPE cells.

This study provides the foundation for exploring whether the conditioned medium of RPE cells and POS could contribute to future strategies for developing functional and mature RPE-like cells derived from BMMSCs. However, there are some limitations that should be considered, particularly with respect to the specific mechanisms of the epithelial–mesenchymal transition (EMT) and mesenchymal–epithelial transition (MET). During routine culture on tissue-culture plastic, RPE cells lose epithelial characteristics and acquire a mesenchymal cell-like phenotype [Grisanti and Guidry, 1995].

In this study, the polygonal cells typical of primary RPE cells were unfortunately absent in all BMMSCs cultures after 7 days and longer of treatment. This suggested the rare effects of the RPECM and POS

on the MET and the difference between the RPE phenotype of the RPECM-POS-treated cultures and RPE in vivo. In addition to the production of soluble factors and pigment granules, cultured RPE cells could have depleted some nutrients or essential factors from the RPECM. Despite these limitations, however, our study highlights the potential for the combination of RPECM and POS to stimulate BMMSCs differentiation toward an RPE phenotype. Future investigations will be required to establish the mechanisms of these effects, including further studies of the MET.

DISCLOSURES

The authors indicate no potential conflicts of interest.

REFERENCES

Alge CS, Suppmann S, Priglinger SG, Neubauer AS, May CA, Hauck S, Welge-Lussen U, Ueffing M, Kampik A. 2003. Comparative proteome analysis of native differentiated and cultured dedifferentiated human RPE cells. Invest Ophthalmol Vis Sci 44:3629–3641.

Arnhold S, Absenger Y, Klein H, Addicks K, Schraermeyer U. 2007. Transplantation of bone marrow-derived mesenchymal stem cells rescue photoreceptor cells in the dystrophic retina of the rhodopsin knockout mouse. Graefes Arch Clin Exp Ophthalmol 245:414–422.

Atmaca-Sonmez P, Li Y, Yamauchi Y, Schanie CL, Ildstad ST, Kaplan HJ, Enzmann V. 2006. Systemically transferred hematopoietic stem cells home to the subretinal space and express RPE-65 in a mouse model of retinal pigment epithelium damage. Exp Eye Res 83:1295–1302.

Bonilha VL, Rodriguez-Boulan E. 2001. Polarity and developmental regulation of two PDZ proteins in the retinal pigment epithelium. Invest Ophthalmol Vis Sci 42:3274–3282.

Castanheira P, Torquetti L, Nehemy MB, Goes AM. 2008. Retinal incorporation and differentiation of mesenchymal stem cells intravitreally injected in the injured retina of rats. Arq Bras Oftalmol 71:644–650.

Chang CW, Roque RS, Defoe DM, Caldwell RB. 1991. An improved method for isolation and culture of pigment epithelial cells from rat retina. Curr Eye Res 10:1081–1086.

Chiou SH, Kao CL, Peng CH, Chen SJ, Tarng YW, Ku HH, Chen YC, Shyr YM, Liu RS, Hsu CJ, Yang DM, Hsu WM, Kuo CD, Lee CH. 2005. A novel in vitro retinal differentiation model by co-culturing adult human bone marrow stem cells with retinal pigmented epithelium cells. Biochem Biophys Res Commun 326:578–585.

Derda R, Li L, Orner BP, Lewis RL, Thomson JA, Kiessling LL. 2007. Defined substrates for human embryonic stem cell growth identified from surface arrays. ACS Chem Biol 2:347–355.

Finnemann SC, Silverstein RL. 2001. Differential roles of CD36 and alphavbeta5 integrin in photoreceptor phagocytosis by the retinal pigment epithelium. J Exp Med 194:1289–1298.

Gal A, Li Y, Thompson DA, Weir J, Orth U, Jacobson SG, Apfelstedt-Sylla E, Vollrath D. 2000. Mutations in MERTK, the human orthologue of the RCS rat retinal dystrophy gene, cause retinitis pigmentosa. Nat Genet 26: 270–271.

Gong L, Wu Q, Song B, Lu B, Zhang Y. 2008. Differentiation of rat mesenchymal stem cells transplanted into the subretinal space of sodium iodate-injected rats. Clin Experiment Ophthalmol 36:666–671.

Grisanti S, Guidry C. 1995. Transdifferentiation of retinal pigment epithelial cells from epithelial to mesenchymal phenotype. Invest Ophthalmol Vis Sci 36:391–405.

Hall MO. 1978. Phagocytosis of light- and dark-adapted rod outer segments by cultured pigment epithelium. Science 202:526–528.

Harris JR, Brown GA, Jorgensen M, Kaushal S, Ellis EA, Grant MB, Scott EW. 2006. Bone marrow-derived cells home to and regenerate retinal pigment epithelium after injury. Invest Ophthalmol Vis Sci 47:2108–2113.

Huang J, Possin DE, Saari JC. 2009. Localizations of visual cycle components in retinal pigment epithelium. Mol Vis 15:223–234.

Hunt RC, Davis AA. 1990. Altered expression of keratin and vimentin in human retinal pigment epithelial cells in vivo and in vitro. J Cell Physiol 145:187–199.

Jaitovich AA, Bertorello AM. 2006. Na^+, K^+-ATPase: An indispensable ion pumping-signaling mechanism across mammalian cell membranes. Semin Nephrol 26:386–392.

Joussen AM, Heussen FM, Joeres S, Llacer H, Prinz B, Rohrschneider K, Maaijwee KJ, van Meurs J, Kirchhof B. 2006. Autologous translocation of the choroid and retinal pigment epithelium in age-related macular degeneration. Am J Ophthalmol 142:17–30.

Li Y, Reca RG, Atmaca-Sonmez P, Ratajczak MZ, Ildstad ST, Kaplan HJ, Enzmann V. 2006. Retinal pigment epithelium damage enhances expression of chemoattractants and migration of bone marrow-derived stem cells. Invest Ophthalmol Vis Sci 47:1646–1652.

Li Y, Atmaca-Sonmez P, Schanie CL, Ildstad ST, Kaplan HJ, Enzmann V. 2007. Endogenous bone marrow derived cells express retinal pigment epithelium cell markers and migrate to focal areas of RPE damage. Invest Ophthalmol Vis Sci 48:4321–4327.

Lin H, Clegg DO. 1998. Integrin alphavbeta5 participates in the binding of photoreceptor rod outer segments during phagocytosis by cultured human retinal pigment epithelium. Invest Ophthalmol Vis Sci 39:1703–1712.

Lutz DA, Guo Y, McLaughlin BJ. 1995. Natural, high-mannose glycoproteins inhibit ROS binding and ingestion by RPE cell cultures. Exp Eye Res 61:487–493.

Marmorstein AD. 2001. The polarity of the retinal pigment epithelium. Traffic 2:867–872.

Marmorstein AD, Finnemann SC, Bonilha VL, Rodriguez-Boulan E. 1998. Morphogenesis of the retinal pigment epithelium: Toward understanding retinal degenerative diseases. Ann NY Acad Sci 857:1–12.

Ohlstein B, Kai T, Decotto E, Spradling A. 2004. The stem cell niche: Theme and variations. Curr Opin Cell Biol 16:693–699.

Pittenger MF, Mackay AM, Beck SC, Jaiswal RK, Douglas R, Mosca JD, Moorman MA, Simonetti DW, Craig S, Marshak DR. 1999. Multilineage potential of adult human mesenchymal stem cells. Science 284:143–147.

Rakoczy P, Kennedy C, Thompson-Wallis D, Mann K, Constable I. 1992. Changes in retinal pigment epithelial cell autofluorescence and protein expression associated with phagocytosis of rod outer segments in vitro. Biol Cell 76:49–54.

Raymond SM, Jackson IJ. 1995. The retinal pigmented epithelium is required for development and maintenance of the mouse neural retina. Curr Biol 5: 1286–1295.

Rosenthal R, Bakall B, Kinnick T, Peachey N, Wimmers S, Wadelius C, Marmorstein A, Strauss O. 2006. Expression of bestrophin-1, the product of the VMD2 gene, modulates voltage-dependent Ca^{2+} channels in retinal pigment epithelial cells. Faseb J 20:178–180.

van Soest S, Westerveld A, de Jong PT, Bleeker-Wagemakers EM, Bergen AA. 1999. Retinitis pigmentosa: Defined from a molecular point of view. Surv Ophthalmol 43:321–334.

Youn YH, Hong J, Burke JM. 2006. Cell phenotype in normal epithelial cell lines with high endogenous N-cadherin: Comparison of RPE to an MDCK subclone. Invest Ophthalmol Vis Sci 47:2675–2685.